Journal of Applied Polymer Science

Graphene Oxide Reinforced Chitosan/Polyvinylpyrrolidone Polymer Bio-Nanocomposites

Mounir El Achaby,[1] Youness Essamlali,[1,2] Nassima El Miri,[1,2] Asmae Snik,[2] Karima Abdelouahdi,[3] Aziz Fihri,[1] Mohamed Zahouily,[1,2] Abderrahim Solhy[1]

[1]Moroccan Foundation for Advanced Science Innovation and Research (MAScIR), Rabat Design, Rue Mohamed El Jazouli, Madinat El Irfane 10100-Rabat, Morocco

[2]Laboratoire de Matériaux, Catalyse et Valorisation des Ressources Naturelles, URAC 24, Faculté des Sciences et Techniques, Université Hassan II-Mohammedia B.P. 146, 20650, Morocco

[3]Division UATRS, Centre National pour la Recherche Scientifique et Technique (CNRST), Angle Allal Fassi/FAR, B.P.8027, Hay Riad, 10000-Rabat, Morocco

Correspondence to: M. El Achaby (E-mail: m.elachaby@mascir.com) and A. Solhy (E-mail: a.solhy@mascir.com)

ABSTRACT: Bio-nanocomposite films based on chitosan/polyvinylpyrrolidone (CS/PVP) and graphene oxide (GO) were processed using the casting/evaporation technique. It has been found that the three components of bio-nanocomposites can be easily mixed in controlled conditions enabling the formation of thick films with high quality, smooth surface and good flexibility. Structural and morphological characterizations showed that the GO sheets are well dispersed in the CS/PVP blend forming strong interfacial interactions that provide an enhanced load transfer between polymer chains and GO sheets thus improving their properties. It has been found that the water resistance of the CS/PVP blend is improved, and the hydrolytic degradation is limited by addition of 0.75 and 2 wt % GO. The modulus, strength, elongation and toughness of the bio-nanocomposites are together increased. Herein, the steps to form new bio-nanocomposite films have been described, taking the advantage of the combination of CS, PVP and GO to design the aforementioned bio-nanocomposite films, which allow to have extraordinary properties that would have promising applications as eventual packaging materials. © 2014 Wiley Periodicals, Inc. J. Appl. Polym. Sci. **2014**, *131*, 41042.

KEYWORDS: biocompatibility; blends; composites; films; graphene and fullerenes; nanotubes

Received 19 March 2014; accepted 17 May 2014
DOI: 10.1002/app.41042

INTRODUCTION

The use of natural polymers for sustainable development and environmental preservation has become ubiquitous in the last 20 years. Therefore many studies have been devoted to the development of polymer bio-nanocomposites, where at least one of the components is derived from nature or even biomass. Natural polymers such as proteins and carbohydrates are widely used as materials for conventional and innovative applications. The use of natural polymers has several advantages compared to their counterparts from synthetics due to their particular properties: non-toxicity, biodegradability, wide availability, and biocompatibility.[1]

The chitosan (CS) is a high molecular weight polysaccharide composed of β-(1,4)-2-acetamido-2-deoxy-D-glucose and β-(1,4)-2-amino-2-deoxy-D-glucose units and can be obtained via deacetylation of chitin.[2] This biopolymer is among the most important natural polymers due to their diverse spectrum of applications ranging from pharmaceuticals to materials science.[3–14] However, some obstacles hinder its extensive use, particularly its relatively lower elongation, low toughness properties, poor hydrolytic stability, high degree of swelling in water, and its relatively poor water vapor barrier characteristics as well as high price compared to conventional plastics.[15,16] In an effort to overcome the scientific and technological challenges issues, faced by the use of this biopolymer to expand its range of applications, several attempts have been made to improve these properties, particularly for the CS-based films. Blending of synthetic polymers with CS has been reported for improving the mechanical and functional properties of CS films.[17–21]

Poly(vinylpyrrolidone), PVP, is a synthetic polymer that has a well-defined structure with an *N*-vinylpyrrolidone monomer connected as a long chain. This polymer has good biocompatibility and non-toxic behavior and can be used in many technical applications.[22] Indeed, due to its brittleness, it was generally developed as a copolymer or blend component with other

polymers to develop new nanocomopsite films.[17,20,23,24] It has been reported that CS and PVP are miscible polymers.[17,25] Hong et al. have reported that the carbonyl groups in the pyrrolidone rings of the PVP can interact with amino and hydroxyl groups present in CS *via* hydrogen bonding formation.[23,25] Indeed, the blending of thereof allows to combine the properties of CS and PVP in CS/PVP blend that may lead to the preparation of new biocompatible and homogeneous blend matrix.[17]

On the other hand, nanocomposite technology using nanofillers such as carbon nanotubes, graphene, clay, and hydroxyapatite with low loading has already been proven as an effective way to produce new materials with specific properties and high performances.[26–32] However, two primordial conditions must be achieved to obtain nanocomposite materials with exceptional properties. The first one is the good dispersion and distribution of nanofillers in the polymeric matrix, and the second one is the high degree of interaction between nanofillers and macromolecular chains of polymers.[33]

On another very important aspect, graphene and graphene oxide (GO) have recently attracted much attention due to their exceptional properties, particularly their high mechanical properties and good biocompatibility.[34–37] The GO is a typical pseudo-two-dimensional oxygen-containing solid in bulk form, possesses functional groups including hydroxyls, epoxides, and carboxyls.[36,38–40] Several studies on this subject (graphene & GO) show that the GO can be used as active biocompatible material with specific applications.[39,41] The chemical groups of GO have a crucial role to improve its dispersion in organic solvents and obviously in polymers.[40,42,43] Additionally, functional side groups bound to the surface of GO may improve the interfacial adhesion between GO and the matrix, similarly to that observed for functionalized carbon nanotube-based nanocomposites.[44]

Incorporation of GO within CS is an active approach for improving the physical and chemical properties of CS biopolymer. Previous works have combined GO nanosheets and CS polymer together at low concentrations to create strong, biodegradable, and biocompatible GO-filled CS nanocomposites.[45–49] This can be achieved because the possible strong interactions between nanosheets and CS and the good dispersion of GO on the molecular scale in CS matrix, as well as the interfacial adhesion, thus significantly increasing properties of the CS-based nanocomposites. Recently, some GO-reinforced polymer blend nanocomposite materials have been prepared. Pandele et al. successfully prepared mechanically strong and biocompatible nanocomposite films based on incorporation of GO in CS–PVA blend.[50] Ma et al. developed bio-nanocomposite films with improved water resistance and tensile properties by combination of CS, oxidized starch, and GO.[51] Rodríguez-Gonzâlez et al. developed bio-nanocomposites of CS−starch, and carboxymethyl cellulose–starch blends reinforced with GO and keratin-grafted GO.[52] From their results, the thermomechanical properties of the blends were significantly improved with addition of modified and unmodified GO. Indeed, due to the great compatibility between CS, PVP, and GO and their mixture in water, the development of films from these components is intended to be of major interest. More recently, Mahmoudi et al. prepared 1 wt % GO filled CS/PVP biocompatible films with tunable optical transparency and gas permeability.[53] Thus, with an aim to make the biopolymers as materials that can be competitive with the fossil derivatives, with high structural and mechanical properties, the researches on GO-filled biocompatible polymers have gained considerable momentum.[42,45,47,48]

Our approach in the present work is to take advantage of complementary properties of the three materials, biocompatibility and non-toxicity associated with CS and PVP and exceptional properties of GO in order to obtain biocompatible and mechanically strong hybrid bio-nanocomposite films by dispersing GO sheets in PVP/CS blend. The effect of addition of GO on the morphology, the structural and mechanical properties as well as the water resistance, hydrolytic degradation and thermal stability of CS/PVP-based bio-nanocomposite films have been evaluated. This proposed method herein provides a new approach to design and prepare the bio-nanocomposite films with expected performance for cutting-edge industries.

EXPERIMENTAL

Materials

CS (Aldrich, high molecular weight with 20% acetylation) and PVP (Aldrich, average molecular weight of 10,000) were used as the polymeric components. Natural powder graphite ($\leq$20 μm, 99.99%), sulfuric acid (99%), hydrochloric acid (37%), acetic acid ($\geq$ 99%), sodium nitrate ($\geq$ 99%), potassium permanganate (99%), and hydrogen peroxide (30%) were purchased from Aldrich and used without further purification.

Preparation

The solvent cast method was used to prepare the films of neat CS, CS/PVP blend, CS/PVP blend filled by 0.75 and 2 wt % GO (Scheme 1). Firstly, 3 g of CS were dissolved in 150 mL of 1% (v/v) aqueous acid acetic solution at ambient temperature with constant stirring for 5 h. Then, 3 g of PVP was separately dissolved in 150 mL of deionized water with constant stirring for 1 h, and the obtained solution of PVP was added into the CS solution, followed by mechanical stirring of 2 h to form CS/PVP (50:50) blend solution. For the preparation of GO-based nanocomposite films, the desired amount (0.75 and 2 wt % in regard to CS/PVP blend) of pre-exfoliated GO dispersion was added to the above CS-PVP mixture followed by sonication (Ultrasonic System, SharperTek® Stamina XP^{TM}, 50 W) for 15 min and continuously stirred to form homogeneous mixture (1 h). The obtained homogeneous mixture was cast onto PET sheets and kept on a hot plate to facilitate fast removal of water. After which, the film was peeled from the sheets and kept in vacuum oven at 100°C for 5 h, for complete removal of water. It should be noted that the exfoliated GO were prepared via chemical oxidation of natural graphite followed by sonication (Ultrasonic System, SharperTek® Stamina XP^{TM}, 50 W) assisted water-phase exfoliation according to our previous works.[40,54] Neat CS and CS–PVP blend films were also similarly prepared as a reference material, without adding the GO. The films are designated as CS for neat Chitosan, CS/PVP for CS/PVP blend, CS/PVP@-0.75 and CS/PVP@-2 for nanocomposites-containing 0.75 and 2 wt % GO, respectively. The film thickness is kept

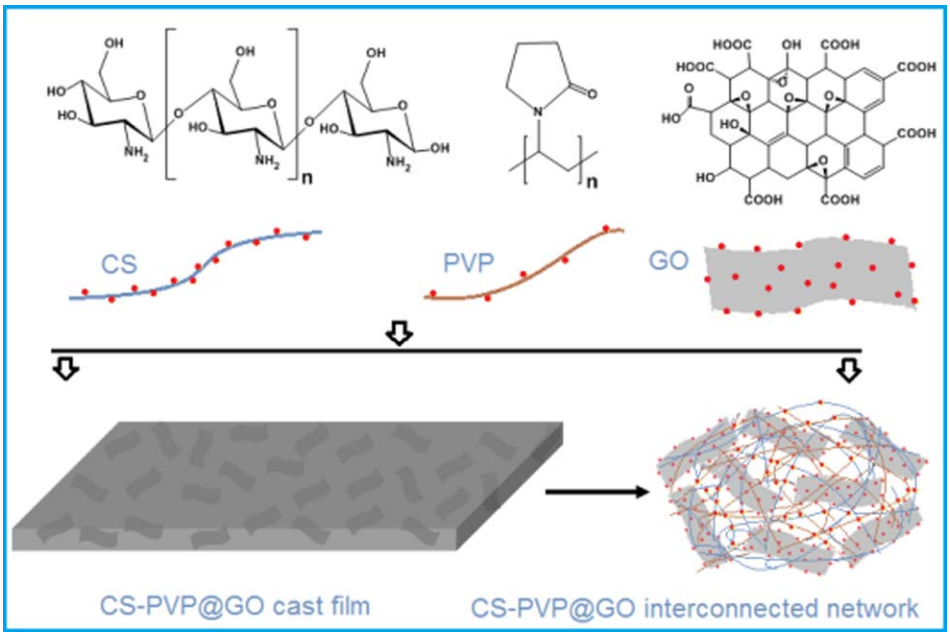

Scheme 1. Schematic representation of the structures of based products (CS, PVP and GO) and their well dispersed bio-nanocomposite cast films. [Color figure can be viewed in the online issue, which is available at wileyonlinelibrary.com.]

uniform (70 μm) for all samples by controlling the amount of film-forming solutions.

Characterization Techniques

Atomic Force Microscopy (AFM) measurements was carried out using a Veeco Dimension ICON. The samples used for AFM characterizations were deposited on mica sheets. TEM micrographs were obtained on a Tecnai G2 microscope at 120 kV. The morphology of solvent-cast films was evaluated from a cryofracture surface, using a scanning electron microscopy (SEM) upon an apparatus: FEI Quanta 200. X-ray diffraction patterns were obtained at room temperature on a Bruker AXS D-8 diffractometer using Cu-Kα radiation in Bragg-Brentano geometry (θ-2θ). In order to avoid the influence of the thickness of specimens, all the samples used for the measurement have a same thickness of 70 μm. Transform Infrared Spectroscopy (FTIR) was performed on an ABB Bomem FTLA 2000 spectrometer equipped with a Golden Gate single reflection ATR accessory. Thermogravimetric analyses (TGA) and derivative thermogravimetry (DTG) were conducted using a TA Instruments Q500 apparatus with 10°C/min ramp between 25 and 700°C under nitrogen. Tensile tests were performed using an Instron 8821S tensiometer. The tensile specimens were cut in rectangular shapes with dimensions of 80 mm in length and 10 mm in width. The gauge length was fixed at 40 mm and the speed of the moving clamp was 10 mm/min. All tests were carried out on a minimum of four samples and the reported results are average values.

To investigate the water absorption degree, the as-prepared films were first dried, accurately weighted and then immersed in distilled water for 12 and 24 h, respectively, at room temperature. The wet weight of the flms was measured by taking out the flms from the water and blotting with a flter paper to remove the surface adsorbed water followed by immediately weighing of these flms.[55] The water uptake or water content (WC) of the flms was calculated according to the following equation:

$$\text{Water content (WC) (\%)} = \frac{(W_f - W_i)}{W_i} \times 100$$

Where W_f and W_i are the weights of the wet films and dry films, respectively.

The hydrolytic degradation tests of the films were performed in distilled water at room temperature for an extended time. Indeed, each film was immersed in water and stored for 30 days. After this time, the residual samples were removed from the water solution and dried at 80°C for 48 h and subsequently weighed to determine their residual mass.

RESULTS AND DISCUSSION

Before blending of suspended GO sheets with CS/PVP polymer blend, the individual GO sheets were obtained by intense sonication in water of completely oxidized natural graphite which is confirmed by TEM and AFM observations.[40] Importantly, the successful oxidation of graphite is crucial for its complete exfoliation into individual GO sheets.[40,56] During this operation, it was noted that the GO dispersion gradually transformed into a yellow brown solution. This is a sign that the graphite oxide powder was transformed into GO sheets. Remarkably, it should be noted that the dispersion of GO was stable even after 4 weeks storage at room temperature [Figure 1(a)]. TEM results confrm the existence of individual GO sheets, as shown in Figure 1(b), which present a typical TEM picture of the GO sheets.

The AFM images of the GO reveal the presence of irregular shaped sheets with uniform thickness and different lateral dimensions (Figure 2). As shown from the height profiles

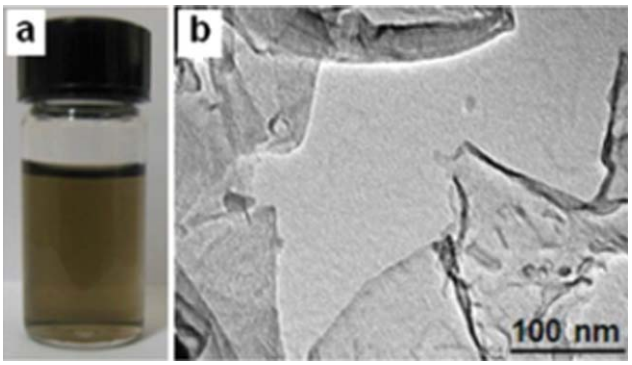

Figure 1. Photograph of exfoliated GO dispersion in water (a), and TEM image of GO sheets (b). [Color figure can be viewed in the online issue, which is available at wileyonlinelibrary.com.]

recorded at different locations, the thickness of obtained sheets is observed at ~1 nm while lateral dimensions range from ~100 to ~800 nm. We conclude from this analysis that no GO sheets are thicker or thinner than 1 nm, which can be explained by the efficient top–down process of the exfoliation of graphite oxide into GO sheets achieved by the ultrasonic treatment. However, we would also point out that a single sheet of graphene is atomically flat with a thickness of 0.34 nm, and the GO sheets are expected to be thicker due to the presence of oxygen-containing functional groups attached on both sides of the graphene sheet and the displacement of the sp3-hybridized carbon atoms slightly above and below the original graphene plane.[30,36] In addition, this relatively increased thickness is owed to the wrinkled and folded structure of sheets that arises during solvent evaporation as a space created between the sheets and substrate. This result is in good agreement with our previous work.[40]

CS, PVP, and GO can be easily mixed in controlled conditions enabling the formation of a homogeneous and stable mixture in aqueous media. It has been reported that the CS and PVP are miscible via a specific interaction between the carbonyl groups in pyrrolidone rings of the PVP and the amino and hydroxyl groups present in CS resulting in the formation of hydrogen bonding (self-assembly processes).[23,25,30] Thus, the polymer blend can produce a new material with specific characteristics, which can be used as a new polymeric matrix for development of nanocomposites.[17,53] By casting solutions of CS, CS/PVP blend, and CS/PVP filled by 0.75 and 2 wt % GO mixtures on flat surface, films with high quality, smooth surface, good flexibility and with 70 μm-thick are produced [Figure 3(a–d)]. We note also that the thickness of these films can be controlled by the amount of the solution used for casting process. Furthermore, it can be simply cut into various desired forms by a special knife. Figure 3 illustrates the digital photographies of CS, CS/PVP, CS/PVP@GO-0.75, and CS/PVP@GO-2 films. We see clearly the difference of the colors between the films prepared by solely the CS and the polymeric matrix CS/PVP one hand, and on the other hand the films prepared by the CS/PVP-based matrix reinforced by the two adopted concentrations of the GO (0.75 and 2 wt %).

To microscopically observe the morphology of GO filled CS/PVP nanocomposite films for investigating the dispersion level of GO within the CS/PVP blend matrix, low and high magnification SEM visualizations were performed for the nanocomposite film-containing 2 wt % GO [Figure 3(e,f)]. One can clearly see that the GO has been successfully exfoliated and uniformly dispersed throughout the polymeric blend matrix. It is seen that the GO sheets are wrapped by macromolecular chains of polymers. Because oxygen-containing groups are found on the surface and edge of GO, the compatibility of GO with CS/PVP blend and the quality of dispersion can be significantly improved. In addition, high magnification images reveal that the sheets are isolated and wrinkled within the matrix [Figure 3(f)]. These observed results indicate a good adhesion between CS/PVP blend and GO sheets. The excellent dispersion of GO in the blend matrix is directly correlated with its effectiveness in improving the properties of nanocomposite films.

In order to determine crystal structure of the films and also to check the exfoliation of GO within the polymeric matrix, we analyzed our samples (CS, PVP, CS/PVP, CS/PVP@GO-0.75, and CS/PVP@GO-2) by X-ray diffraction (Figure 4). The XRD

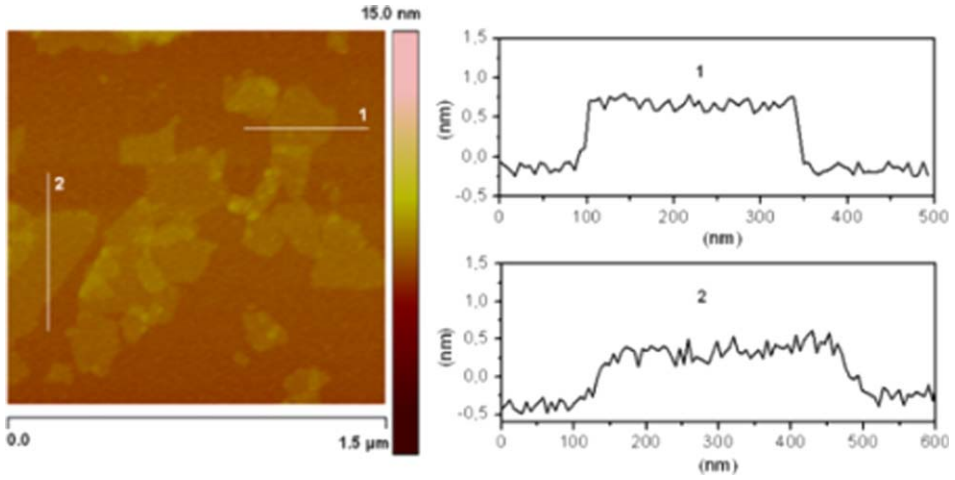

Figure 2. AFM image taken in tapping mode and the corresponding line profiles of exfoliated GO nanosheets deposited from a dispersion in water onto mica substrate. [Color figure can be viewed in the online issue, which is available at wileyonlinelibrary.com.]

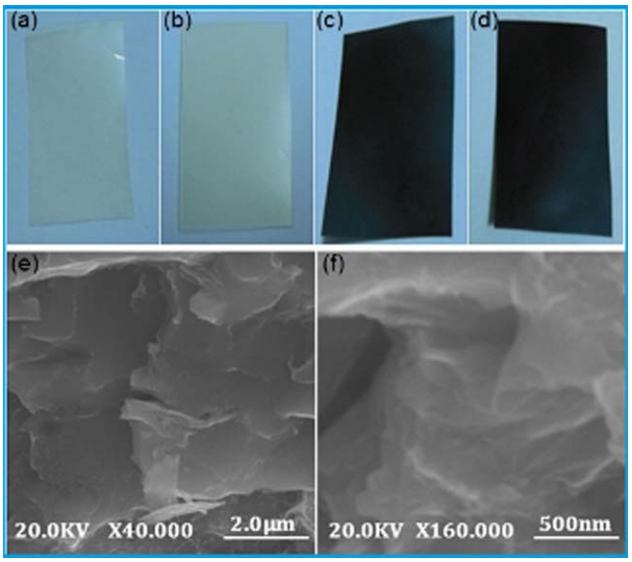

Figure 3. Photographs of isolated films of CS (a), CS/PVP (b), CS/PVP@GO-0.75 (c) and CS/PVP@GO-2 (d) and low (e) and high (f) magnification SEM images of fracture surface of CS/PVP@GO-2 bio-nanocomposite film. [Color figure can be viewed in the online issue, which is available at wileyonlinelibrary.com.]

characterizations of CS revealed the presence of the broad peaks at around 8.4, 11.3, 18.2, and 23°. The first two peaks correspond to the hydrated crystalline structure, whereas the broadened peak at about 23° indicates the existence of an amorphous structure.[46] Similarly, the XRD pattern of the PVP showed the presence of broad peaks between 12–15° and 19–24°, which indicated the amorphous nature of PVP.[57] XRD analysis of the CS/PVP blend shows that the structure is semicrystalline and the sharp peaks observed around 12–15° and 19–24°, indicating the average intermolecular distance of the amorphous part regenerated from the PVP. Importantly, the XRD analysis of CS/PVP@GO-0.75 and CS/PVP@GO-2 bio-nanocomposites revealed the absence of the peak corresponding to GO (2θ =10°), which can be indicated that GO is totally exfoliated in CS/PVP matrix. In addition, the high compatibility between GO and the CS/PVP matrix is responsible for limiting the rearrangement of sheets into layered structure of graphite oxide. Moreover, after addition of GO, the bio-nanocomposite films show a structure similar to that of CS/PVP blend, indicating that the structure of bio-nanocomposites is not influenced by GO.

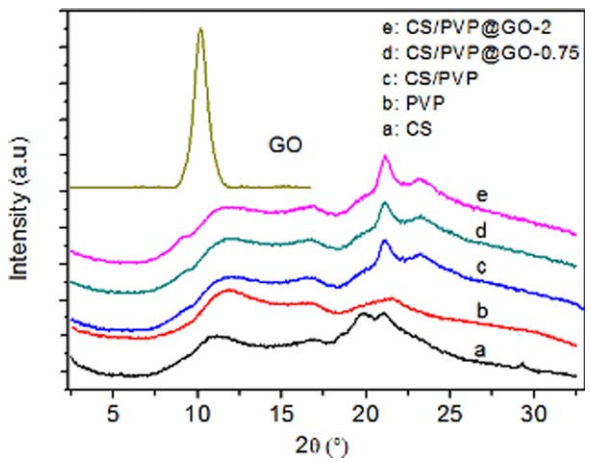

Figure 4. XRD patterns of CS, PVP, CS/PVP blend, CS/PVP@GO-0.75, and CS/PVP@GO-2 bio-nanocomposite films and unexfoliated GO powder. [Color figure can be viewed in the online issue, which is available at wileyonlinelibrary.com.]

Figure 5 shows the FTIR spectra of CS, PVP, CS/PVP blend, and CS/PVP filled by GO. For CS spectrum, the band at 3422 cm^{-1} is associated to O—H and N—H hydrogen band stretches. The bands at 2921 and 2867 cm^{-1} are attributed to C—H stretching. Then, the band at 1653 cm^{-1} is due to C—O

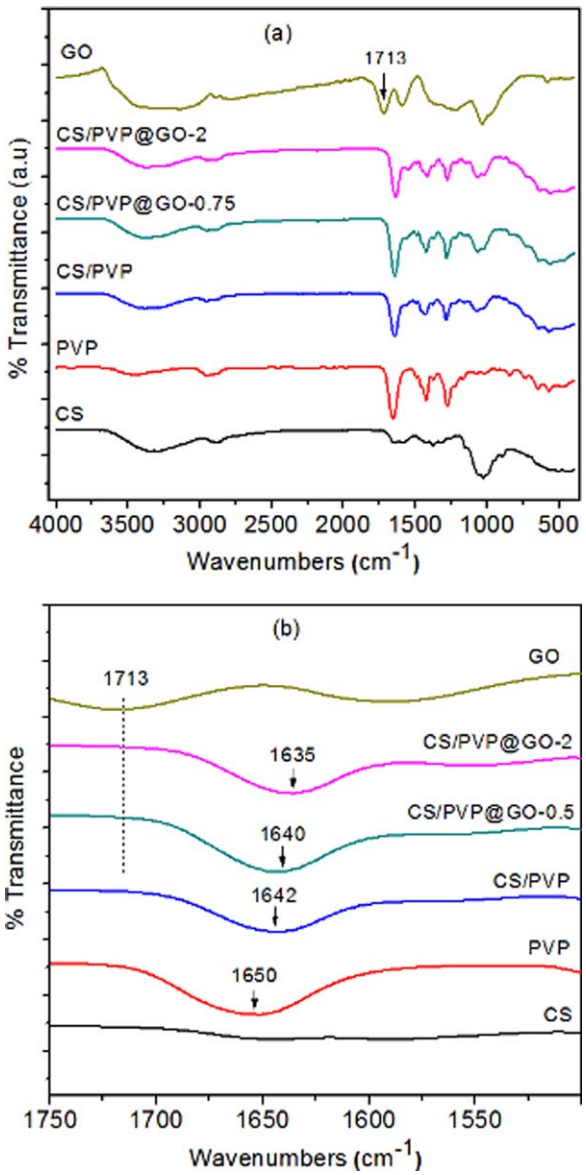

Figure 5. FTIR spectra of CS, PVP, CS/PVP blend, CS/PVP@GO-0.75, and CS/PVP@GO-2 bio-nanocomposite films and GO powder in the region of 400–4000 cm^{-1} (a) and 1500–1750 cm^{-1} (b). [Color figure can be viewed in the online issue, which is available at wileyonlinelibrary.com.]

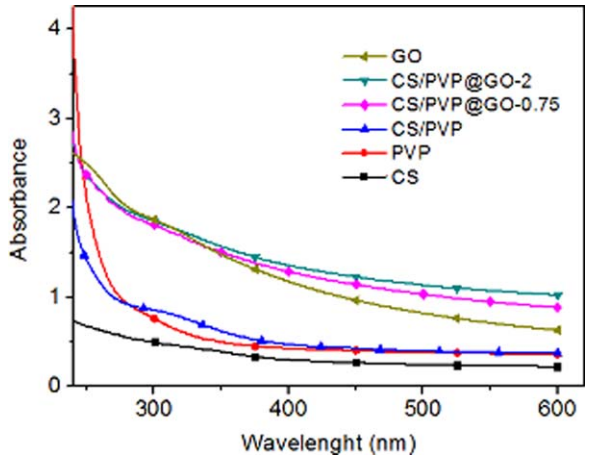

Figure 6. UV-Vis spectra of CS, PVP, CS/PVP blend, CS/PVP@GO-0.75, and CS/PVP@GO-2 bio-nanocomposite films and GO dispersion in water. [Color figure can be viewed in the online issue, which is available at wileyonlinelibrary.com.]

stretching of the acetyl group. The band at 1592 cm^{-1} is associated to N—H bending and stretching. The bands at 1480–1375 cm^{-1} are associated to asymmetrical C—H bending of CH_2 group and the band at 1071 cm^{-1} is associated to the skeletal vibration involving the bridge C—O stretch of glucosamine residue [Figure 5(a)].[58] On the other hand, the FTIR spectrum of the PVP revealed firstly two peaks found at 2962 and 1427 cm^{-1} which be attributed, respectively, to C—H stretching vibrations in aliphatic compounds and to C—H bending vibration from methylene group. Other absorption bands found at 1650 cm^{-1}, 1280 cm^{-1}, and 848 cm^{-1}, which are associated to the stretching vibration of the carbonyl group (C═O), the stretching vibration of the pyrrolidone structure (C—N) and the bending vibration of ═C—H, respectively.[59] Indeed, in the case of the polymeric matrix CS/PVP, we find that the carbonyl band is shifted towards lower frequencies with a single band at 1642 cm^{-1}, which may be due to the existence of the interactions between CS and PVP [Figure 5(b)]. The bands in region of 3300–3500 cm^{-1} are usually assigned to the inter- and intramolecular hydrogen bonding of hydroxyl groups.[23] It is possible that the carbonyl groups of PVP can take part in the formation of hydrogen bonding with hydroxyl group of CS at the expense of the hydrogen bonding interaction in CS.[23] Hydroxyl groups of CS were hydrogen donors in forming hydrogen bonding with carbonyl groups of PVP.[23] Furthermore, the FTIR spectra of CS/PVP@GO-0.75 and CS/PVP@GO-2 revealed some important information concerning the interactions between different oxygenated groups present in GO and CS/PVP blend. The C═O carbonyl stretch of the carboxylic group observed at 1713 cm^{-1} in the GO spectrum disappeared in the bio-nanocomposite films indicating that a strong electrostatic interations and hydrogen bonding between the carboxyl group of GO and the amino and hydroxyl groups present in the CS/PVP blend were achieved.[46] The hydroxyl groups of GO observed at 3370 cm^{-1} and 1370-1150 cm^{-1} can also interact with the non-interacting carbonyl groups of PVP in the CS/PVP blend. This interaction is possible because the carbonyl group frequency is more shifted to lower frequency (1635 cm^{-1}) in CS/PVP blend filled by 2 wt % GO compared to CS/PVP blend [Figure 5(b)]. Based upon the above experimental observations, it can be stated that CS and PVP are perfectly compatible and miscible polymers *via* the hydrogen bond interactions between carbonyl groups of PVP and equal part of amino and hydroxyl groups of the CS. When the GO is added to CS/PVP blend, additional hydrogen bonding can occurs between the carboxylic acid groups of GO and amino and hydroxyl groups of CS and between the hydroxyl groups of GO and the carbonyl groups of PVP. Therefore, an interconnected structure is assumed to be formed in CS/PVP filled by GO originated from the strong interactions between the macromolecular chains of polymers and the sheets of GO (Scheme 1).

The structure and the optical absorption of the films were also studied by UV-vis absorption (Figure 6). Evidently, no absorption peak was observed for the CS and PVP polymers since these polymers are know to be transparent in the UV-visible region. For the CS/PVP blend, there is a weak absorbance about 300–350 nm may be due to the interaction between the CS and the PVP. For the CS/PVP@GO-0.75 and CS/PVP@GO-2 bio-nanocomposite films, the strengthening by addition of GO sheets has the further consequence that the bio-nanocomposite films becoming darker corresponding to a relative increase in the absorbance level for the full wavelength range (Figure 6). Importantly, the lateral size of GO sheets is more than 100 nm, as visualized by AFM observation (Figure 2), their presence in the bio-nanocomposite films is responsible for scatterring and/or absorbing the light and for reducing the optical transparency (increasing of absorbance) of these films based on the CS/PVP blend and GO sheets.[40] On the other hand, no strong scattering and/or absorbing are observed, indicating that the GO are well dispersed at nanoscale within the CS/PVP blend. This is directly related to strong interfacial interactions between the macromolecular chains of the polymers and the surface of GO.

The thermal stability of the studied films is evaluated by TGA–DTG analysis (Figure 7). From the curves presented in Figure 7(a), the degradation of CS film under inert atmosphere indicated an initial weight loss at 50–100°C which associated to the water and the moisture removal. Then, two losses were observed at around 200–300 and 350–600°C, with maximum temperature values of 293 and 554°C in DTG curves [Figure 7(b)], respectively, which could be attributed to the degradation of CS segments. For neat PVP, the absorbed water is first removed at a temperature around 50–100°C after which the complete mass loss occurs between 350 and 470°C, with a maximum temperature of 434°C.[59] The CS–PVP blend decomposes following a three major steps process. The first (250–350°C) and third (525–600°C) steps is due to the decomposition of the components of CS, with maximum temperatures of 296 and 556°C, respectively. The second step (400–475°C) is due to the decomposition of PVP molecules, with a maximum temperature of 445°C. It is noted that, in comparison with neat CS and PVP, the shift in the maximum temperature of degradation of CS and PVP in the blend is due to the strong interaction between them *via* the hydrogen bond interactions between the carbonyl groups of PVP and amino and hydroxyl groups of CS, as deduced from FTIR analysis (Figure 5).

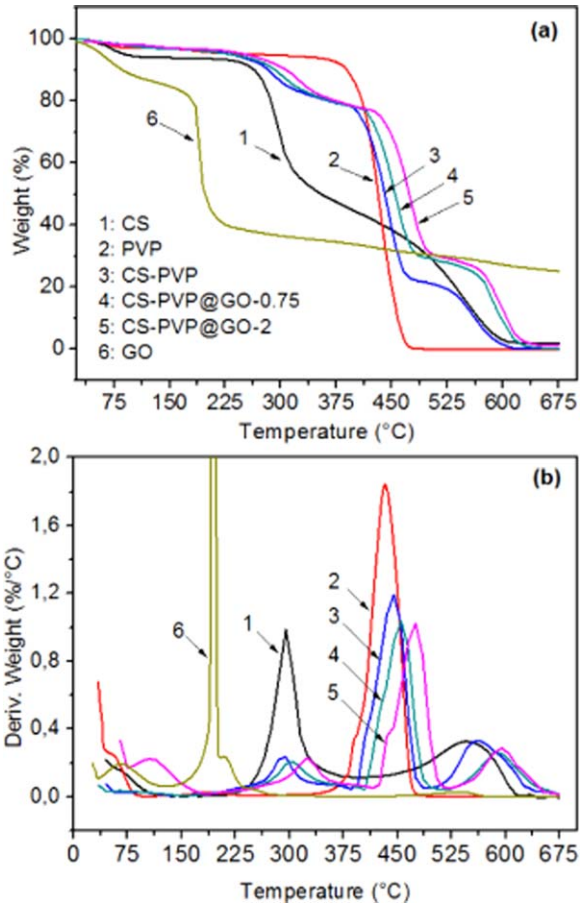

Figure 7. (a) TGA and (b) DTG curves of CS, PVP, CS/PVP blend, CS/PVP@GO-0.75, and CS/PVP@GO-2 bio-nanocomposite films and GO powder. [Color figure can be viewed in the online issue, which is available at wileyonlinelibrary.com.]

The decomposition of GO is done in two steps, the first one was observed in the range of 50–100°C which can be assigned to the loss of absorbed water, whereas the second one was observed around 150–210°C (maximium temperature of 195°C) corresponding to the decomposition of the various oxygen-containing groups.[40] However, the TGA analysis of both bio-nanocomposite films, CS/PVP@GO-0.75 and CS/PVP@GO-2, reveals that the degradation of these films is similar to that observed for unloaded CS/PVP blend (three steps of degradation). It is noted that the major mass loss of GO (~50%), that occurring at a maximium temperature of 195°C, disappeared in the case of bio-nanocomposite films. This can be explained by the strong interaction between the surface functional groups of GO and the macromolecular chains of CS and PVP, what has already been proved through the analysis by the FTIR. Moreover, the maximium temperatures of degradation of bio-nanocomposite films is shifted toward the high temperatures in regard to CS/PVP blend, with a maximium temperatures of degradation of 305, 454, and 583°C for CS/PVP@GO-0.75 and 326, 475, and 596°C for CS/PVP@GO-2, identified in the three steps of degradation, which gives advantage to improve the thermal stability of these bio-nanocomposite films [Figure 7(b)]. This can be explained by a possible mobility suppression of the CS/PVP segments at the interface between macromolecular chains and GO sheets.

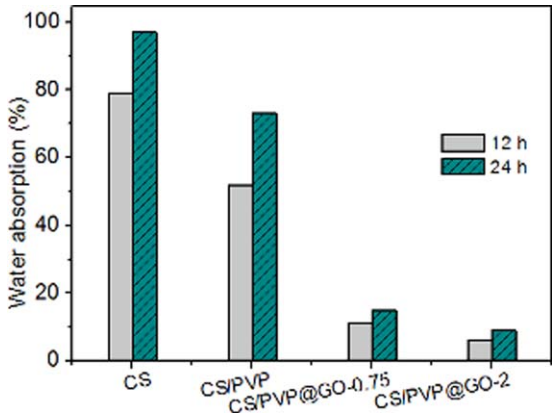

Figure 8. Water absorption of CS, CS/PVP blend, CS/PVP@GO-0.75, and CS/PVP@GO-2 bio-nanocomposite films recorded for 12 and 24 h in water. [Color figure can be viewed in the online issue, which is available at wileyonlinelibrary.com.]

Figure 8 illustrates the water absorption percentages that correspond to the water uptake or WC of CS, CS/PVP, CS/PVP@GO-0.75, and CS/PVP@GO-2 films. It is clear that the addition of PVP significantly reduces the WC percentage of CS/PVP film. The WC values of the pure CS flm after immersion in water for 12 and 24 h were measured at 79 and 97%, respectively, whereas the WC values of the CS/PVP blend do not exceed 52 and 73% after immersion in water for 12 and 24 h, respectively. When GO was added to the CS/PVP blend, this percentage was reduced to 11 and 15% for CS/PVP@GO-0.75, and 6 and 9% for CS/PVP@GO-2 after immersion in water for 12 and 24 h, respectively. It is clear that the presence of GO within the CS/PVP blend may further limit the absorption of water by the bio-nanocomposite films. In general, water uptake of the bio-nanocomposite flms depends on the nature of the matrix and fller. This phenomenon of reduced water uptake at equilibrium can be ascribed to the formation of strong fller–matrix interactions.[55] The well dispersed sheets acted as an interpenetrated network within the CS/PVP blend matrix (Scheme 1) and prevented the swelling of the flms when exposed to water.

The hydrolytic degradation behavior in water-based environment of CS, CS/PVP, and CS/PVP@GO films is further evaluated to study the effect of addition of PVP polymer and GO nanosheets on the long-term hydrolytic degradation of CS-based film in water media. Figure 9 shows the photographs of neat CS, CS/PVP blend and CS/PVP@GO-2 films immersed in water. The photographs are taken 5 min [Figure 5(a–c)] and 30 days [Figure 9(d–f)] after immersion of the films in water and their state just after removal of water after 30 days [Figure 9(g–k)]. It is well known that the CS film is an unstable material in wet environment.[47] This behavior is also observed in this work, while the neat CS film is apparently degraded and broken in the form of many small pieces [Figure 5(d–g)]. This is primarily due to the presence of amine and hydroxyl groups on the CS

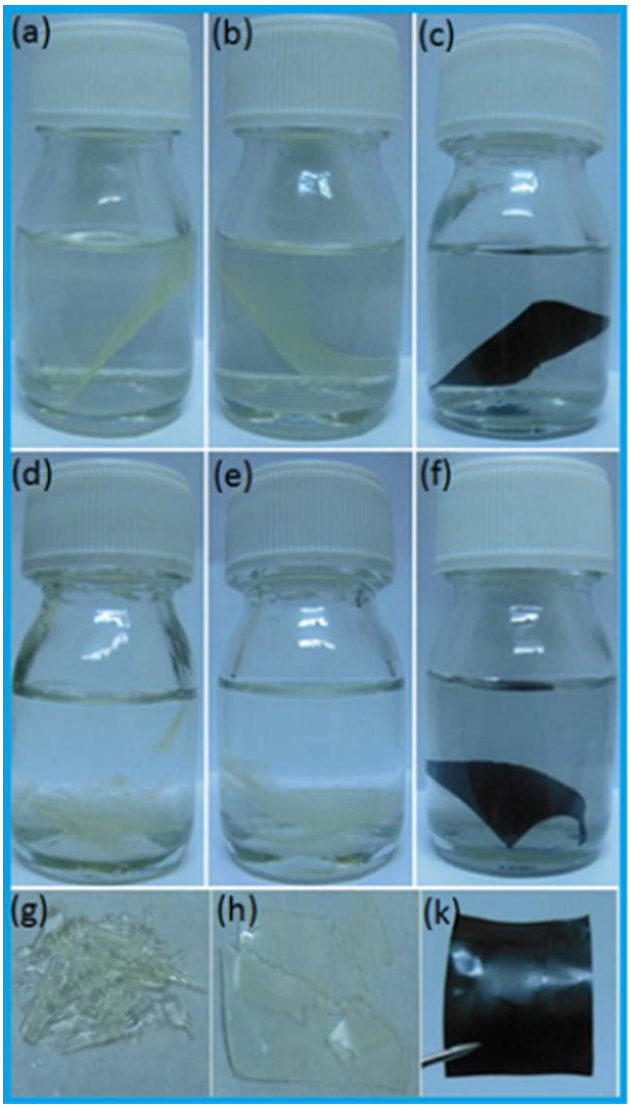

Figure 9. Photographs of CS (a,d,g), CS/PVP blend (b,e,h), and CS/PVP@GO-2 (c,f,k). The photographs are taken 5 min (a,b,c) and 30 days (d,e,f) after immersion of the films in water and their state just after removal of water after 30 days (g,h,k). [Color figure can be viewed in the online issue, which is available at wileyonlinelibrary.com.]

moiety, which are the most probable sites that have a high affinity for water.

This visual hydrolytic degradation of CS film is significantly decreased when 50 wt % of PVP is added. As mentioned before, the water uptake of CS/PVP blend is significantly lower than that of neat CS film (Figure 8), and this leads to increased hydrolytic degradation of the neat CS. Indeed, when PVP is blended with CS, the amine and hydroxyl groups of CS can therefore interact with the carbonyl groups of PVP, resulting in the formation of a compact tri-dimensional network in the blend and the affinity of CS for water is reduced. These results would indicate that there was minimal degradation, as shown in Figure 9(e,h), while the CS/PVP blend film is broken in some large pieces in comparison with those observed for neat CS film [Figure 9(g)]. The reduced hydrolytic degradation of CS/PVP

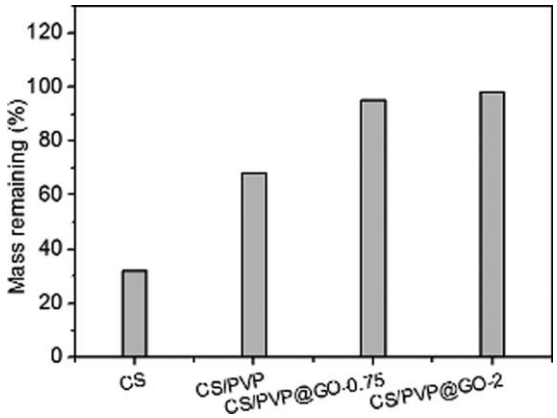

Figure 10. Mass remainning of CS, CS/PVP blend, CS/PVP@GO-0.75, and CS/PVP@GO-2 bio-nanocomposite films after a degradation time of 30 days.

blend indicates that some non-interacting amine, hydroxyl, and carbonyl groups are still presented in the formed material (CS/PVP), which is responsible on the reaction with water, resulting in hydrolysis mechanism. Besides, after addition of GO into CS/PVP blend, more interactions are occurred between the non-interacting groups of CS/PVP blend and the oxygenated groups of GO, as confirmed by FTIR analysis (Figure 5). Thus, for the CS/PVP@GO-2 film, there is no visual hydrolytic degradation occurs and the bio-nanocomposite flm is still in a whole with strength [Figure 9(f,k)]. Similar result is previously reported in the literature for 3 wt % GO filled neat CS nanocomposite film prepared by solvent casting method.[47]

Figure 10 shows the values of the residual mass measured for each sample after removal of water and drying for a degradation time of 30 days. From this Figure, the mass remaining of the neat CS is about 32%, indicating that the major mass of CS is degraded underwater attack. For the CS/PVP blend, we observed a significant difference in degradation behavior compared with the neat CS, while the mass remaining is measured at 68%. In this case, the water shows a little ability for degradation mechanism, because the CS and PVP are well blended, thus the possibility of the degradation decreased. In the case of CS/PVP@GO-0.75 film, there is only a small weight loss during 30 days, while the mass remaining is about 95%. More specially, no weight loss was observed for the bio-nanocomposite-containing 2 wt % GO (CS/PVP@GO-2), leaving a mass remaining of 98%, indicating that the presence of GO in the CS/PVP blend has a clear delaying effect on the hydrolytic degradation of CS/PVP-based bio-nanocomposite films. This behavior can be explained in terms of the homogeneity of dispersion/distribution of GO, which creates a tortuous path for the penetration of water and limits the hydrolytic degradation of the produced bio-nanocomposites. As results, the addition of GO into the CS/PVP could significantly limit the hydrolytic degradation of the formed bio-nanocomposite flms, which is attracting for its potential application as packing material.

The mechanical properties of the films of neat CS, CS/PVP blend, CS/PVP@GO-0.75, and CS/PVP@GO-2 were investigated by uniaxial tensile tests. From the stress–strain curves (results

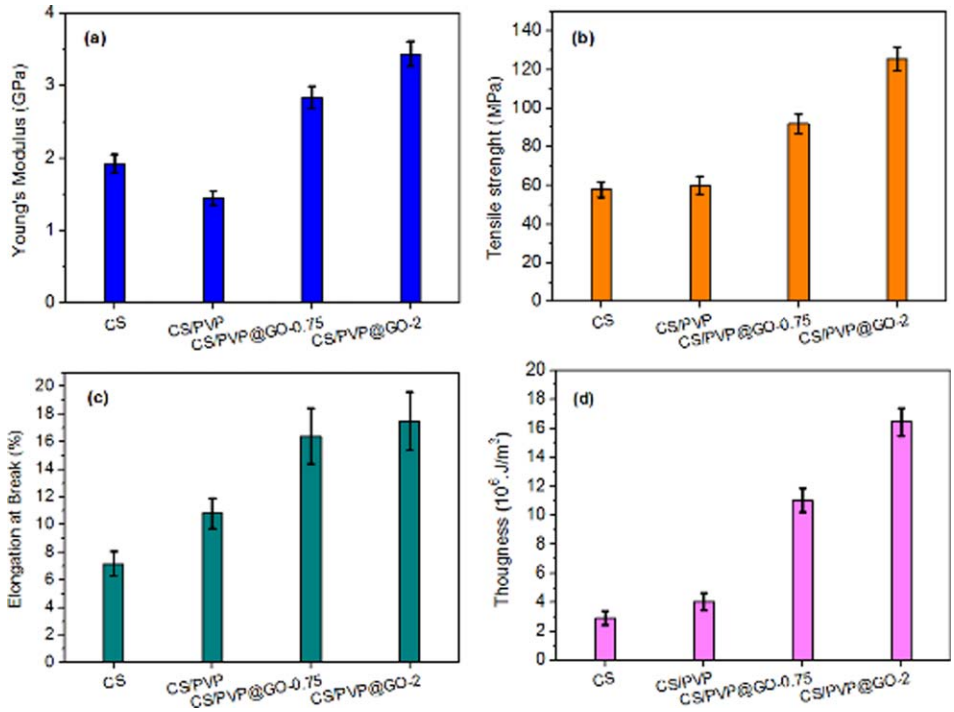

Figure 11. Tensile properties of CS, CS/PVP blend, CS/PVP@GO-0.75, and CS/PVP@GO-2: (a) Young's modulus, (b) Tensile strength, (c) Elongation at break, and (d) Toughness. [Color figure can be viewed in the online issue, which is available at wileyonlinelibrary.com.]

not shown here), the elongation at break (ε_b), the ultimate tensile strength (σ_s), the Young's modulus (E) and the toughness (T) of the studied films are extracted and presented in Figure 11. The Young's modulus [Figure 11(a)] can be defined as the slope of the linear elastic deformation of the stress–strain curve, the Ultimate tensile strength [Figure 11(b)] represents the maximum stress value applied to the material, the elongation at break [Figure 11(c)] is defined as the strain to break of the material, and the toughness [Figure 11(d)] is the energy needed to break the material, and can be calculated from the area under the stress–strain curve.

From the results illustrated in Figure 11, i is clear that the selected tensile properties of CS are affected by its blending with 50% PVP and then by addition of 0.75 and 2 wt % of GO sheets. Due to the cristallinity nature and low molecular weight of CS biopolymer, its solvent casted film is mechanically brittle material. The CS film has an elongation at break of 7.16%, ultimate tensile stress of 57.9 MPa, Young's modulus of 1.92 GMPa and toughness of 2.92×10^6 J m^{-3} (Figure 11). These selected tensile properties of the CS flm were affected when a 50% of PVP is added. Indeed, the elongation at break is increased up to 10.8% for CS/PVP blend, indicating that this film become more ductile in comparison with CS film. The increase of elongation at break is accompanied by an increase of the ultimate tensile strength up to 60.1 MPa and the toughness up to 4.04×10^6 J m^{-3}. These slight changes are due to the formation of a tri-dimensional network in the blend that generated from the strong interactions between the CS and PVP. On the other hand, the Young's modulus is decreased after addition of PVP, because this polymer have a lower intrinsic stiffness in comparison with that of CS bipolymer. More importantly, for the addition of GO nanosheets within the CS/PVP blend, a remarkable increase in elongation at break, strength, modulus and toughness is clearly visible (Figure 11). This could be due to the formation of more compact network that generated from the addition of GO nanosheets within the CS–PVP blend (Scheme 1). The tensile strength and Young's modulus of the CS/PVP@GO increased by 109% from 60.1 to 125.5 MPa [Figure 11(a)] and by 130% from 1.45 to 3.34 GPa [Figure 11(b)], respectively, when 2 wt % GO is added into the CS/PVP blend. This trend has been also reported in the literature for GO filled CS bio-nanocomposite films.[46,47, 60–62] Such improvements confirm that GO filled CS/PVP blend are mechanically strong material. Furthermore, it should be pointed out that the CS/PVP@GO films not have only a higher strength and modulus but also a higher elongation at break, in comparaison with the uncharged CS/PVP blend. This is unusual, as most graphene filled CS nanocomposites become brittle with addition of even small amounts of graphene.[45,47] In some cases, simultaneously improved tensile strength, Young's modulus and elongation at break of CS-based nanocomposites have been reported, with incorporation of graphene or functionalized graphene into CS polymer.[41,48] More specially, the elongation at break of the CS/PVP@GO film is about 17.5%, which is an increase of 62 % in comparison with uncharged CS/PVP blend film [Figure 11(d)]. The extended elongation at break as well as the toughness observed for GO reinforced films confirm that these films are mechanically flexible. Apparently, the large aspect ratio and very high Young's modulus of GO are responsible on the significant reinforcement impact on mechanical properties of the CS/PVP blend. In addition, homogeneous dispersion of GO along with the favorable interfacial interactions between GO and the

polymeric blend are the key points to achieve final tensile properties improvement for these bio-nanocomposite films. It is suggested that films suitable for food packaging should preferably strong and flexible. This trend is observed for the GO-based bio-nanocomposite films fabricated in the present work.

CONCLUSION

High performance novel polymer bio-nanocomposite films were prepared *via* solution casting of CS, polyvinylpyrrolidone (PVP), and GO. The structural characterizations show that the CS and PVP are perfectly compatible and miscible polymers *via* the hydrogen bond interactions between the carbonyl groups of PVP and amino and hydroxyl groups of CS, resulting in the formation of new biocompatible homogeneous blend matrix for bio-nanocomposite development. When the GO has been added to CS/PVP blend, some additional hydrogen bonding can occurs between the carbonyl groups of carboxylic acid in GO and amino and hydroxyl groups of CS and between the hydroxyl groups of GO and the carbonyl groups of PVP. Therefore, an interconnected structure is assumed to be formed in CS/PVP strengthened by GO. Since that the special two-dimensional morphology of the GO as well as its functionalized surface provides well homogeneous dispersion, which leads to a high contact area in the CS/PVP matrix. This was mainly the result of a strong interaction between the macromolecular chains of polymers and the sheets of GO. Owing to these strong interfacial interactions, large improvements of certain properties, such as water resistance, hydrolytic degradation, and tensile properties were achieved for CS/PVP-based bio-nanocomposite films. With the incorporation of 2 wt % GO, the water uptake percentage is reduced to 9% after 24h immersion in water, and the weight loss during 30 days immersion in water is limited. In addition, the modulus, strength, elongation and toughness of CS/PVP filled by 2% GO were increased by 130, 109, 62, and 464%, respectively. Therefore, the as-prepared bio-nanocomposite films with features of high stiffness, good flexibility and high water-resistance will have potential applications as an eventual food packaging materials.

ACKNOWLEDGMENTS

The financial assistance of the Office Chérifien des Phosphates in the Moroccan Kingdom toward this research is hereby acknowledged. We equally thank the technical support team of the MAScIR Foundation. We gratefully acknowledge Dr. Abdelkarim El Kadib, senior researcher at euromed university in Morocco, for his help to achieve this work. The authors also acknowledge Mr. Chakib Tilsaghani, director of platforms at MAScIR Foundation.

REFERENCES

1. Raemdonck, K.; Martens, T. F.; Braeckmans, K.; Demeester, J.; De Smedt, S. C. *Adv. Drug Deliv. Rev.* **2013**, *65*, 1123.
2. Rogovina, S. Z.; Alexanyan, C. V.; Prut, E. V. *J. Appl. Polym. Sci.* **2011**, *121*, 1850.
3. Klinkesorn, U. *Food Rev. Int.* **2013**, *29*, 371.
4. El Kadib, A.; Molvinger, K.; Bousmina, M.; Brunel, D. *J. Catal.* **2010**, *273*, 147.
5. Vauthier, C.; Zandanel, C.; Ramon, A. L. *Curr. Opin. Colloid Interface Sci.* **2013**, *18*, 406.
6. Shukla, S. K.; Mishra, A. K.; Arotiba, O. A.; Mamba, B. B. *Int. J. Biol. Macromol.* **2013**, *59*, 46.
7. Dutta, P. K.; Tripathi S.; Mehrotra, G. K.; Dutta, J. *Food Chem.* **2009**, *114*, 1173.
8. Albanna, M. Z.; Bou-Akl, T. H.; Blowytsky, O.; Walters, H. L.; Matthew, H. W. T. *J. Mech. Behav. Biomed.* **2013**, *20*, 217.
9. Vasconcellos, F. C.; Goulart, G. A. S.; Beppu, M. M. *Powder Technol.* **2011**, *205*, 65.
10. Ma, J.; Sahai, Y. *Carbohydr. Polym.* **2013**, *92*, 955.
11. Jayakumar, R.; Prabaharan, M.; Nair, S. V.;Tokura, S.; Tamura, H.; Selvamurugan, N. *Prog. Mater. Sci.* **2010**, *55*, 675.
12. Dash, M.; chiellini, F.; Ottenbrite, R. M.; chiellini, E. *Prog. Mater. Sci.* **2011**, *36*, 981.
13. Céline, P-B.; Antoine, V.; Denis, B.; Laurent, V.; Laurent, D.; Catherine, F. *J. Appl. Polym. Sci.* **2013**, *128*, 2945.
14. Hassan, M. L.; Fadel, S. M.; El-Wakil, N. A.; Oksman, K. *J. Appl. Polym. Sci.* **2012**, *125*, E216.
15. Butler, B. L.; Vergano P. J.; Testin, R. F.; Bunn, J. M.; Wiles, J. L. *J. Food Sci.* **1996**, *61*, 953.
16. Park, S. Y.; Marsh, K. S.; Rhim, J. W. *J. Food Sci.* **2002**, *67*, 194.
17. Yeh, J-T.; Chen, C-L.; Huang, K. S.; Nien, Y. H.; Chen, J. L.; Huang, P. Z. *J. Appl. Polym. Sci.* **2006**, *101*, 885.
18. Rajan, M.; Raj, V. *Carbohydr. Polym.* **2013**, *98*, 951.
19. Yu, H.; Xu, X.; Chen, X.; Hao, J.; Jing, X. *J. Appl. Polym. Sci.* **2006**, *101*, 2453.
20. Archana, D.; Singh, B. K.; Dutta, J.; Dutta, P. K. *Carbohydr. Polym.* **2013**, *95*, 530.
21. Devi, D. A.; Smitha, B.; Sridhar, S.; Aminabhavi, T. M. *J. Membr. Sci.* **2006**, *280*, 45.
22. Xiaoli, L.; Yajun, X.; Zhaoqiang, W.; Hong, C. *Macromol. Biosci.* **2013**, *13*, 147.
23. Wang, B.; Wang, J.; Li, D.; Ren, K.; Ji, J. *Appl. Surf. Sci.* **2012**, *258*, 7801.
24. Ummartyotin, S.; Bunnak, N.; Juntarob, J.; Sain, M.; Manuspiya, H. C. R. *Phys. Physique* **2012**, *13*, 994.
25. Hong, Y.; Chirila, T. V.; Vijayasekaran, S.; Shen, W.; Lou, X.; Dalton, P. *J. Biomed. Mater. Res.* **1998**, *39*, 650.
26. Liu, D.; Zhang, Y.; Sun, X.; Chang, P. R. *J. Appl. Polym. Sci.* **2014**, *131*, 40359.
27. El Achaby, M., Qaiss, A. *Mater. Des.* **2013**, *44*, 81.
28. Kango, S.; Kalia, S.; Celli, A.; Njuguna, J.; Habibi, Y.; Kumar, R. *Prog. Polym. Sci.* **2013**, *38*, 1232.
29. Du, Y.; Shen, S. Z.; Cai, K.; Casey, P. S. *Prog. Polym. Sci.* **2012**, *37*, 820.
30. Sionkowska, A. *Prog. Polym. Sci.* **2011**, *36*, 1254.
31. El Achaby, M.; Ennajih, H.; Arrakhiz, F. Z.; El Kadib, A.; Bouhfd, R.; Essassi, E.; Qaiss A. *Compos. B* **2013**, *51*, 310.

32. Lim, S. K.; Kim, J. W.; Chin, I., Kwon; Y. K.; Choi, H. *J. Chem. Mat.* **2002**, *14*, 1989.
33. Mittal, V. *Macromol. Mater. Eng.* **2014**, DOI: 10.1002/mame.201300394.
34. Yoo, B. M.; Shin, H. J.; Yoon, H. W.; Park, H. B. *J. Appl. Polym. Sci.* **2014**, *131*, 39628.
35. Ramanathan, T.; Abdala, A. A.; Stankovich, S.; Dikin, D. A.; Herrera-Alonso, M.; Piner, R. D.; Adamson, D. H.; Schniepp, H. C.; Chen, X.; Ruoff, R. S.; Nguyen, S. T.; Aksay, I. A.; Prud'- Homme, R. K., Brinson, L. C. *Nat. Nanotechnol.* **2008**, *3*, 327.
36. Stankovich, S.; Dikin, D. A.; Piner, R. D.; Kohlhaas, K. A.; Kleinhammes, A.; Jia, Y.; Wu, Y.; Nguyen, S. T.; Ruoff, R. S. *Carbon* **2007**, *45*, 1558.
37. Chen, W.; Yan, L.; Bangal, P. R. *Carbon* **2010**, *48*, 1146.
38. Schniepp, H. C.; Li, J. L.; McAllister, M. J.; Sai, H.; Alonso, M. H.; Adamson, D. H. *J. Phys. Chem. B.* **2006**, *110*, 8535.
39. Stankovich, S., Dikin; D. A.; Dommett, G. H. B.; Kohlhaas, K. M.; Zimney, E. J.; Stach, E. A.; Piner, R. D.; Nguyen, S. T.; Ruoff, R. S. *Nature* **2006**, *442*, 282.
40. El Achaby, M.; Arrakhiz, F-E.; Vaudreuil, S.; Essassi, E.; Qaiss, A. *Appl. Surf. Sci.* **2012**, *258*, 7668.
41. Wang, K.; Ruan, J.; Song, H.; Zhang, J.; Wo, Y.; Guo, S.; Cui, D. *Nanoscale Res. Lett.* **2011**, *6*, 1.
42. Layek, R. K.; Kundu, A.; Nandi, A. K. *Macromol. Mater. Eng.* **2013**, *298*, 1166.
43. Parades, J. I.; Villar-Rodil, S.; Martinez-Alonso, A.; Tascon, J. M. D. *Langmuir* **2008**, *24*, 10560.
44. Coleman, J. N.; Cadek, M.; Blake, R.; Nicolosi, V.; Ryan, K.; Belton, C.; Fonseca, A.; Nagy, J.; Gun'ko, Y.; Blau, W. *Adv. Funct. Mater.* **2004**, *14*, 791.
45. Fan, H.; Wang, L.; Zhao, K.; Li, N.; Shi, Z.; Ge, Z.; Jin, Z. *Biomacromolecules* **2010**, *11*, 2345.
46. Yang, X.; Tu, Y.; Li, L.; Shang, S.; Tao, X. *ACS Appl. Mater. Interfaces* **2010**, *6*, 1707.
47. Han, D.; Yan, L.; Chen, W.; Li, W. *Carbohydr. Polym.* **2011**, *83*, 653.
48. Justin, R.; Chen, B. *Carbohydr. Polym.* **2014**, *103*,70.
49. Chen, Y.; Qi, Y.; Yan, X.; Ma, H.; Chen, J.; Liu, B.; Xue, Q. *J. Appl. Polym. Sci.* **2014**, *131*, 40006.
50. Pandele, A. M.; Ionita, M.; Crica, L.; Dinescu, S.; Costache, M.; Iovu, H. *Carbohydr. Polym.* **2014**, *102*, 813.
51. Ma, J.; Liu, C.; Li, R.; Wang, J. *J. Appl. Polym. Sci.* **2012**, *123*, 2933.
52. Rodríguez-González, C.; Martínez-Hernández, A. L.; Castaño, V. M.; Kharissova, O. V.; Ruoff, R. S.; Velasco-Santos, C. *Ind. Eng. Chem. Res.* **2012**, *51*, 3619.
53. Mahmoudi, N.; Ostadhossein, F.; Simchi, A. Chitosan/ Polyvinyl Pyrrolidone/Nano-layer Graphene Oxide Biocompatible Films for Food Packaging. Proceedings of the 5th International Conference on Nanostructures (ICNS5), Kish Island, Iran, March 6–9, **2014**;
54. El Achaby, M.; Arrakhiz, F. E.; Vaudreuil, S.; Qaiss, A.; Bousmina, M.; Fassi-Fehri, O. *Polym. Compos.* **2012**, *33*, 733.
55. Khan, A.; Khan, R. A.; Salmieri, S.; Tien, C. L.; Riedl, B.; Bouchard, J.; Chauve, G.; Tan, V.; Kamal, M. R.; Lacroix, M. *Carbohydr. Polym.* **2012**, *90*, 1601.
56. El Achaby, M.; Arrakhiz, F-E.; Vaudreuil, S.; Essassi, E.; Qaiss, A.; Bousmina, M. *J. Appl. Polym. Sci.* **2013**, *127*, 4697.
57. Ramya, C. S.; Selvasekarapandian, S.; Savitha, T.; Hirankumar, G.; Angelo, P. C. *Phys. B.* **2007**, *393*, 11.
58. Singh, V.; Sharma, A. K.; Tripathi, D. N.; Sanghi, R. *J. Hazard. Mater.* **2009**, *161*, 955.
59. El Achaby, M.; Arrakhiz, F-E.; Vaudreuil, S.; Essassi, E.; Qaiss, A.; Bousmina, M. *Polym. Eng. Sci.* **2013**, *53*, 34.
60. Layek, R. K.; Samanta, S.; Nandi, A. K. *Polymer* **2012**, *3*, 2265.
61. Ryu, H-J.; Mahapatra, S. S.; Yadav, S. K.; Cho, J. W. *Eur. Polym. J.* **2013**, *49*, 2627.
62. Pan, Y.; Wu, T.; Bao, H.; Li, L. *Carbohydr. Polym.* **2011**, *83*, 1908.